

# Assessment and modeling of NH<sub>3</sub>-SnO<sub>2</sub> interactions using individual nanowire sensors

F. Shao<sup>1</sup>, F. Hernandez-Ramirez<sup>1,2</sup>, J.D. Prades<sup>2</sup>, J.R. Morante<sup>1,2</sup>, Thomas Fischer<sup>3</sup>, Sanjay Mathur<sup>3</sup>, Nuria Lopez<sup>4</sup>

1. Catalonia Institute for Energy Research, IREC, Jardins de les Dones de Negre 1, 08930 Sant Adrià de Besòs, Barcelona, Spain

2. University of Barcelona, UB, Martí i Franquès 1, 08028 Barcelona, Spain

3. Institute of Inorganic Chemistry, University of Cologne, 50939 Cologne, Spain

4. Institute of Chemical Research of Catalonia, ICIQ, Av. Països Catalans 16, 43007 Tarragona, Spain  
fhernandez@irec.cat

## Abstract:

In this work, DFT (density functional theory) calculations were applied to study the interaction between NH<sub>3</sub> and the SnO<sub>2</sub> surface. To that end, two types of scenarios were selected; (i) the clean stoichiometric SnO<sub>2</sub> (110) surface and (ii) a SnO<sub>2</sub> (110) surface with pre-adsorbed O<sub>ads</sub>. The NH<sub>3</sub> adsorption mechanism and charge transfer to the metal oxide after the adsorption and dissociation steps of the molecule were simulated to gain a deeper insight into the NH<sub>3</sub> sensing mechanism of this metal oxide. Making use of the intrinsic advantages of nanoscale prototypes, the analysis of the nanowires' resistance modulation upon exposure to NH<sub>3</sub> and their dynamic response, as function of temperature and gas concentration, allowed validating some of the theoretical results.

**Key words:** NH<sub>3</sub>, SnO<sub>2</sub>, Nanowire, Model

## Introduction

SnO<sub>2</sub> as sensing material has been widely used in solid state metal oxide gas sensors due to the low cost and good sensitivity [1,2]. When used as a sensor, the resistance of SnO<sub>2</sub> usually decreases in response to reducing gases, and in general, the gas response has been considered to be the result of charge transfers either directly between adsorbed molecules and the surface or indirectly between the surface and the products of surface reactions involving the pre-adsorbed oxygen species [3, 4]. This second mechanism is believed to be the origin of NH<sub>3</sub> detection with SnO<sub>2</sub>. Nevertheless, it remains not fully understood from a theoretical and experimental point of view.

Different from more studied gases such as O<sub>2</sub>[5], H<sub>2</sub>O[6] and CO[7], our knowledge about the behavior of NH<sub>3</sub> onto the SnO<sub>2</sub> surface is still limited. Temperature Programmed Desorption (TPD) experiments performed by Abee and Cox [8] concluded that NH<sub>3</sub> adsorbs on the 5-coordinated Sn site on the stoichiometric surface with the desorption temperature at around 250K. On the other hand, the Sn4c is a stronger adsorption site

when there are bridging oxygen vacancies available. The desorption peak for the Sn4c is at around 470K. UPS experiment reported by the same author validated the charge transfer from the NH<sub>3</sub> molecule to the metal oxide surface.

On the side of theoretical simulation, the interaction of NH<sub>3</sub> with the MOX surface and metal decorated MOX is highly interesting for heterogeneous catalysis [9-11]. Nevertheless, no literature about the adsorption of this molecule and further reactions onto SnO<sub>2</sub> has been published to the best of our knowledge. Only similar DFT calculations have been reported for NH<sub>3</sub> adsorption on TiO<sub>2</sub>[12], ZnO[13] and RuO[11].

In parallel, the adsorption of oxygen (O) on SnO<sub>2</sub> surface has been demonstrated by many different TPD works, and the ionic charge states has been proved by Electron Spin Resonance (ERS) experiments. However, the existence of atomic charged O<sup>-</sup> on SnO<sub>2</sub> has been questioned by A. Gurlo [14] due to the lack of direct spectroscopic evidence. Oxygen adsorption and dissociation have been intensively studied [16, 17] by using ab-initio methods, and the common results from these

works are: (i) molecular oxygen ( $O_2$ ) only adsorbs to the reduced  $SnO_2$  (110) surface and (ii) atomic O adsorbent can be produced on top of  $Sn_{5c}$  sites following the dissociation step at the  $O_b$  vacancy. In more recent DFT studies [5], calculated adsorption energy was successfully correlated with previous experimental evidences for the different charged oxygen species including atomic  $O^-$ .

In this work, we studied the adsorption of  $NH_3$  onto (i) the clean stoichiometric  $SnO_2$  (110) surface and (ii)  $SnO_2$  surface with  $O_{ads}$  pre-adsorbed after healing an oxygen vacancy. Charge density difference analyses were performed for several critical steps and interactions to study the electronic property changes associated with the  $NH_3$ - $SnO_2$  activity.

### Computational and experimental methods and details

DFT calculations were performed with the Vienna ab initio simulation Package (VASP) [18, 19] using the generalized gradient approximation [20] (GGA). The core electrons were represented by projector-augmented wave [21] (PAW) potentials. Revised-Perdew-Burke-Ernzerhof [22] (r-PBE) functional was employed to treat the exchange correlation potentials. Plane wave cut off energy of 400eV was applied throughout the work. The surface slab containing 5  $SnO_2$  (110) layers and having a  $(2 \times 1)$  periodicity of surface unit cell was applied. A 10Å vacuum layer was placed between the slabs to eliminate the interaction between them. K-point sampling was set to  $4 \times 4 \times 1$  for the surface slab and  $1 \times 1 \times 1$  for the molecules in vacuum adopting the Monkhorst-Pack grids (Fig.1). Geometry relaxation was performed until the energy change of electronic step goes under  $1 \times 10^{-5}$ eV and ionic step below  $1 \times 10^{-4}$ eV. The top three layers of atoms were allowed to move in the relaxation. The accuracy of current model has been verified in previous works [23]. Spin polarization was enabled when free electrons were present.

$NH_3$  adsorption profiles were calculated on the clean and O pre-adsorbed stoichiometric surface with one O atom binding to the  $Sn_{5c}$  site. The atomic O in the latter case is assumed to be generated by the  $O_2$  dissociation which heals the  $O_{2c}$  vacancy at the same time. These two surfaces properly simulate the non-perfect  $SnO_2$  surface existing in real conditions.

The adsorption energy is given by equation:

$$E_{ads} = E_{tot} - E_{sur} - E_{ad}, \quad (i)$$

where  $E_{tot}$  is the ground state energy of surface with adsorbed molecule,  $E_{sur}$  is the energy of the initial surface and  $E_{ad}$  is that for a gas

molecule in vacuum. Therefore, a negative value of  $E_{ads}$  indicates the adsorption at 0K.

To analyze the influence of  $NH_3$  adsorption and dissociation to the electronic property of  $SnO_2$ , charge density difference was calculated applying following equation:

$$\Delta\rho = \rho_{sub+ads} - \rho_{sub} - \rho_{ads} \quad (ii)$$

where  $\rho_{sub+ads}$  represents the charge density of the complete surface system and  $\rho_{sub}$ ,  $\rho_{ads}$  the charge density of the substrate and the adsorbate, respectively.  $\rho_{sub}$ ,  $\rho_{ads}$  were obtained from the same atomic structures and space coordinates as those in the relaxed molecule on surface system.

$SnO_2$  nanowires grown by CVD were used to fabricate the tested prototypes. Individual nanowires were electrically contacted by direct Focused-Ion-Beam (FIB) platinum deposition, using a FEI Dual-Beam Strata 235 instrument combined with a metallorganic injector to deposit platinum. Electrical measurements were performed using a Keithley 2400 Source Meter Unit (SMU). For gas sensing experiments, the devices were placed in a Linkam chamber with an integrated heater; the gas flow ( $\geq 99.999\%$  purity) was regulated by mass flow controllers.

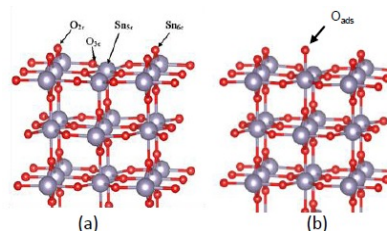


Figure.1. (a) Clean stoichiometric surface of  $SnO_2$  (110), (b)  $SnO_2$  (110) surface with  $O_{ads}$

### Results

$SnO_2$  (110) has four kinds of surface atoms:  $Sn_{5c}$ ,  $Sn_{6c}$ , bridging  $O_{2c}$  and in-plane  $O_{3c}$  (Fig.1). The  $Sn_{5c}$  is considered to be a Lewis acid site which is able to withdraw electrons from an electron rich atom, e.g. N, in the case of  $NH_3$ . In addition, DFT calculations of  $NH_3$  adsorption on other MOX have shown that bonding happens between the unsaturated metal and the N atom of  $NH_3$ . Our searching for adsorption profile of ammonia onto tin oxide confirms this point: the adsorption occurs onto the  $Sn_{5c}$  site, with Sn-N bond perpendicular to the surface plane, as shown in Fig.2(a). The adsorption energy was found to be -1.14eV. The other considered adsorption geometries included the N binding to the  $O_{3c}$  and the H binding to  $O_{3c}$ . Adding a

second  $\text{NH}_3$  on the other  $\text{Sn}_{5c}$  site to imitate the 100% coverage reduced the average  $E_{\text{ads}}$  to  $-0.73\text{eV}$ . The lateral interaction between the adsorbed molecules was concluded from such decrease.

On the other hand, the  $E_{\text{ads}}$  of a  $\text{NH}_3$  molecule onto the remaining  $\text{Sn}_{5c}$  of the surface with pre-adsorbed  $\text{O}_{\text{ads}}$  was found to be  $-1.58\text{eV}$ . This value is  $0.44\text{eV}$  larger than on the clean stoichiometric surface. The  $\text{O}_{\text{ads}}$  had its bond with  $\text{Sn}_{5c}$   $5.3^\circ$  tilted from the surface normal and the distance from the  $\text{O}_{\text{ads}}$  to the closest H of  $\text{NH}_3$  was found to be  $1.98 \text{ \AA}$ , indicating the presence of hydrogen bonding.

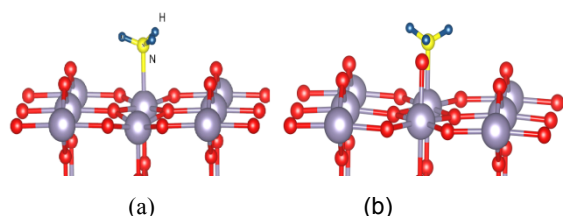


Fig. 2. (a) Adsorption geometries of a  $\text{NH}_3$  molecule onto a clean stoichiometric surface and (b) onto a surface with pre-adsorbed  $\text{O}_{\text{ads}}$

Charge density difference was calculated for several critical structures to evaluate the charge redistribution on the surface region induced by molecule adsorption and dissociation. As shown in Fig. 3. (a), the cyan color indicates the decrease of charge density in the bottom of the N atom and on top of  $\text{Sn}_{5c}$  while the yellow color indicates the increase of charge density between the N and  $\text{Sn}_{5c}$  and at the upper part of the N. This kind of charge distribution is the typical character of covalent bond. Also, charge polarization was found on the in-plane  $\text{O}_{3c}$ .

On the clean stoichiometric surface, charge transfer between  $\text{O}_{2c}$  and two underneath  $\text{Sn}_{6c}$  atoms was able to see. Charge is drawn from the  $\text{Sn}_{6c}$  to the  $\text{O}_{2c}$ . When  $\text{H}_2\text{O}_{2c}$  is formed, less amount of charge transfer was indicated by the smaller iso-surface value. It is a similar situation with the  $\text{O}_{\text{ads}}$  on the  $\text{Sn}_{5c}$ ; charge density difference figure showed the ionic character of the bonding and charge transfer from the surface to  $\text{O}_{\text{ads}}$ . When  $\text{H}_2\text{O}_{\text{ads}}$  was formed, the smaller volume inside the iso-surface on  $\text{Sn}_{5c}$  atom suggested less amount of charges are transferred.

Over all, drawing of charges from surface happened with the adsorption of  $\text{NH}_3$ , O ion and oxidation of an  $\text{O}_{2c}$  vacancy. Nevertheless,  $\text{NH}_3$  was not a charge donator to the surface and adsorption of  $\text{NH}_3$  itself on surface did not generate the sensing effect we experimentally measured. Forming  $\text{H}_2\text{O}$  and the later desorption from the surface returned the

electrical charges to surface and reduced the resistance of the material.

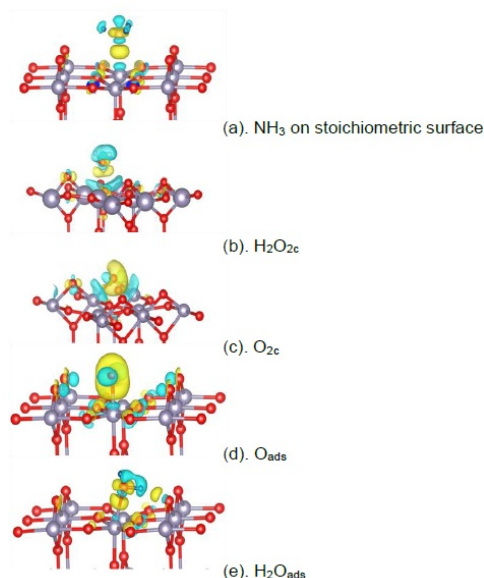


Fig. 3. charge density difference plot, iso-surface: (a), (c), (d), (e):  $0.005\text{e}/\text{Br}^3$ , (b):  $0.002\text{e}/\text{Br}^3$

Confronting experimental data (Fig. 4) with ab-initial DFT simulations, the main  $\text{NH}_3$ - $\text{SnO}_2$  sensing characteristics were validated. This analysis will be presented in this contribution.

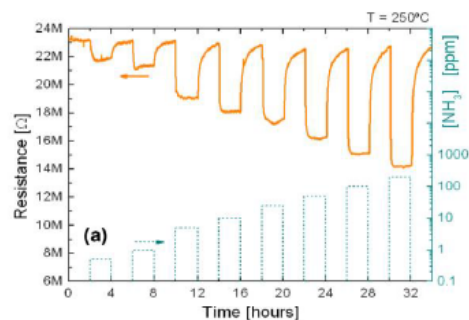


Fig. 4. Nanowire response towards sequential pulses of ammonia (500 ppb to 200 ppm) in synthetic air at a temperature of  $250^\circ\text{C}$

## Conclusion

In summary, the adsorption sites of  $\text{NH}_3$  on clean  $\text{SnO}_2$  stoichiometric surface and a surface with pre-adsorbed oxygen  $\text{O}_{\text{ads}}$  have been successfully identified. The adsorption energy was found to be larger with the  $\text{O}_{\text{ads}}$  presence. The charge density difference analysis showed that  $\text{NH}_3$  is not a charge donator to the surface. The sensing effect of  $\text{SnO}_2$  towards  $\text{NH}_3$  could be induced by the  $\text{H}_2\text{O}$  formation and desorption either with the  $\text{O}_{2c}$  or the  $\text{O}_{\text{ads}}$  as all these processes reduce the amount of charges drawn from surface.

## Acknowledgements

The research is supported by the Framework 7 program under the project S3 (FP7-NMP-2009-247768) and the European Regional Development Funds (ERDF, FEDER Programa Competitivitat de Catalunya 2007-2013)

## References

- [1] J. Huang, Q. Wan, Gas Sensors Based on Semiconducting Metal Oxide One-Dimensional Nanostructures, *sensors*, 9 (2009) 9903–9924.
- [2] S.K. Pandey, K.-H. Kim, K.-T. Tang, A review of sensor-based methods for monitoring hydrogen sulfide, *TrAC Trends in Analytical Chemistry*, 32 (2012) 87–99.
- [3] N. Barsan, U. Weimar, Conduction model of metal oxide gas sensors, *J. Electroceram.*, 7 (2001) 143–167.
- [4] M. Batzill, U. Diebold, The surface and materials science of tin oxide, *Prog. Surf. Sci.*, 79 (2005) 47–154.
- [5] M. Habgood, N. Harrison, An ab initio study of oxygen adsorption on tin dioxide, *Surface science*, (2008) 1072–1079.
- [6] D. Koziej, N. Barsan, U. Weimar, J. Szuber, e. al., Water- oxygen interplay on tin dioxide surface: implication on gas sensing, *Chemical Physics Letters*, (2005) 321–323.
- [7] N. Bârsan, U. Weimar, Understanding the fundamental principles of metal oxide based gas sensors; the example of CO sensing with SnO<sub>2</sub> sensors in the presence of humidity *J. Phys.: Condens. Matter* 15 (2003) R813.
- [8] M.W. Abee, D.F. Cox, NH<sub>3</sub> chemisorption on stoichiometric and oxygen-deficient SnO<sub>2</sub>(110) surfaces, *surface science*, (2002) 65–77.
- [9] R.M. Yuan, G. Fu, X. Xu, H.L. Wan, Mechanisms for Selective Catalytic Oxidation of Ammonia over Vanadium Oxides, *Journal of Physical Chemistry C*, (2011) 21218–21229.
- [10] D.J. Cheng, J.H. Lan, D.P. Cao, W.C. Wang, Adsorption and dissociation of ammonia on clean and metal-covered TiO<sub>2</sub> rutile (110) surface: A comparative DFT study, *Applied Catalysis B: Environmental*, (2011) 510–519.
- [11] J. Perez-Ramirez, N. Lopez, E.V. Kondratenko, Pressure and materials effects on the selectivity of RuO<sub>2</sub> in NH<sub>3</sub> oxidation, *J. Phys. Chem. C*, 114 (2010) 16660.
- [12] I. Onal, S. Soyer, S. Senkan, Adsorption of water and ammonia on TiO<sub>2</sub>-anatase cluster models, *Surf. Sci.*, (2006) 2457–2469.
- [13] Q.Z. Yuan, Y.P. Zhao, L.M. Li, T.H. Wang, Ab Initio Study of ZnO<sub>2</sub> Based Gas Sensing Mechanisms: Surface Reconstruction and Charge Transfer, *J. Phys. Chem. C*, (2009) 6107–6113.
- [14] A. Gurlo, Interplay between O<sub>2</sub> and SnO<sub>2</sub>: Oxygen Ionosorption and Spectroscopic Evidence for Adsorbed Oxygen, *CHemPhysChem*, 7 (2006) 2041– 2052.
- [15] T. Sahm, A. Gurlo, N. Barsan, U. Weimar, Basics of oxygen and SnO<sub>2</sub> interaction: work function change and conductivity measurements, *Sens. Actuators: B*, 118 (2006).
- [16] J. Oviedo, M.J. Gillan, First-principles study of the interaction of oxygen with the SnO<sub>2</sub> (110) surface, *Surf. Sci.*, (2001) 221–236.
- [17] W. Wei, Y. Dai, B.B. Huang, Role of Cu Doping in SnO<sub>2</sub> Sensing Properties Toward H<sub>2</sub>S, *J. Phys. Chem. C*, 115 (2011) 18597–18602.
- [18] G. Kresse, J. Hafner, Ab initio molecular dynamics for liquid metals, *Physics review B*, 47 (1993) 558.
- [19] G. Kresse, J. Furthmüller, Efficient iterative schemes for ab initio total-energy calculations using a plane-wave basis set, *Physical Review B*, 54 (1996) 11169–11186.
- [20] J.A. White, D.M. Bird, Implementation of gradient-corrected exchange-correlation potentials in Car-Parrinello total-energy calculations, *Physical Review B*, 50 (1994) 4954–4957.
- [21] G. Kresse, D. Joubert, From ultrasoft pseudopotentials to the projector augmented-wave method, *Physical Review B*, 59 (1999) 1758–1775.
- [22] B. Hammer, L.B. Hansen, J.K. Nørskov, Improved adsorption energetics within density-functional theory using revised Perdew-Burke-Ernzerhof functionals, *Physical Review B*, 59 (1999) 7413–7421.
- [23] N. Lopez, J.D. Prades, F.H. Ramirez, J.R. Morante, S. Mathur, Bidimensional versus tridimensional oxygen vacancy diffusion in SnO<sub>2-x</sub> under different gas environments, *Phys. Chem. Chem. Phys.*, 12 (2010) 2401.